



*Supplement of*

**Modelling the deep convective transport of trace gases  
(CO, NH<sub>3</sub> and SO<sub>2</sub>) from the planetary boundary layer to  
the Asian summer monsoon anticyclone**

**Jianzhong Ma et al.**

*Correspondence to:* Jianzhong Ma ([majz@cma.gov.cn](mailto:majz@cma.gov.cn)) and Qianshan He ([oxeye75@163.com](mailto:oxeye75@163.com))

The copyright of individual parts of the supplement might differ from the article licence.

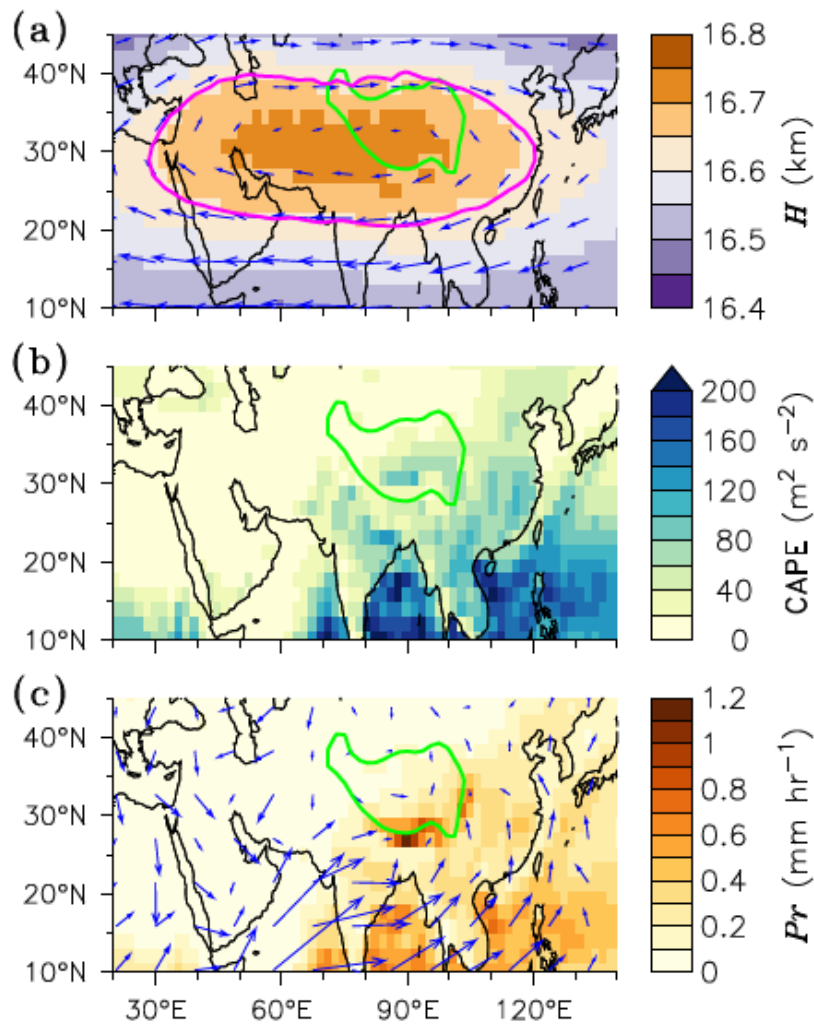


**Figure S1.** EMAC simulated geopotential height above sea level ( $H$ ) with the wind field overlaid (represented by vectors) at 100 hPa (a), convective available potential energy (CAPE), a metric of the atmospheric instability (b), and precipitation rate ( $Pr$ ) (c), averaged for JJA over the years 2010-2020. The purple line in (a) shows the 16.64 km geopotential height contour, highlighting the main anticyclone area. Green lines represent the 3 km terrain-contour height, highlighting the Tibetan Plateau.

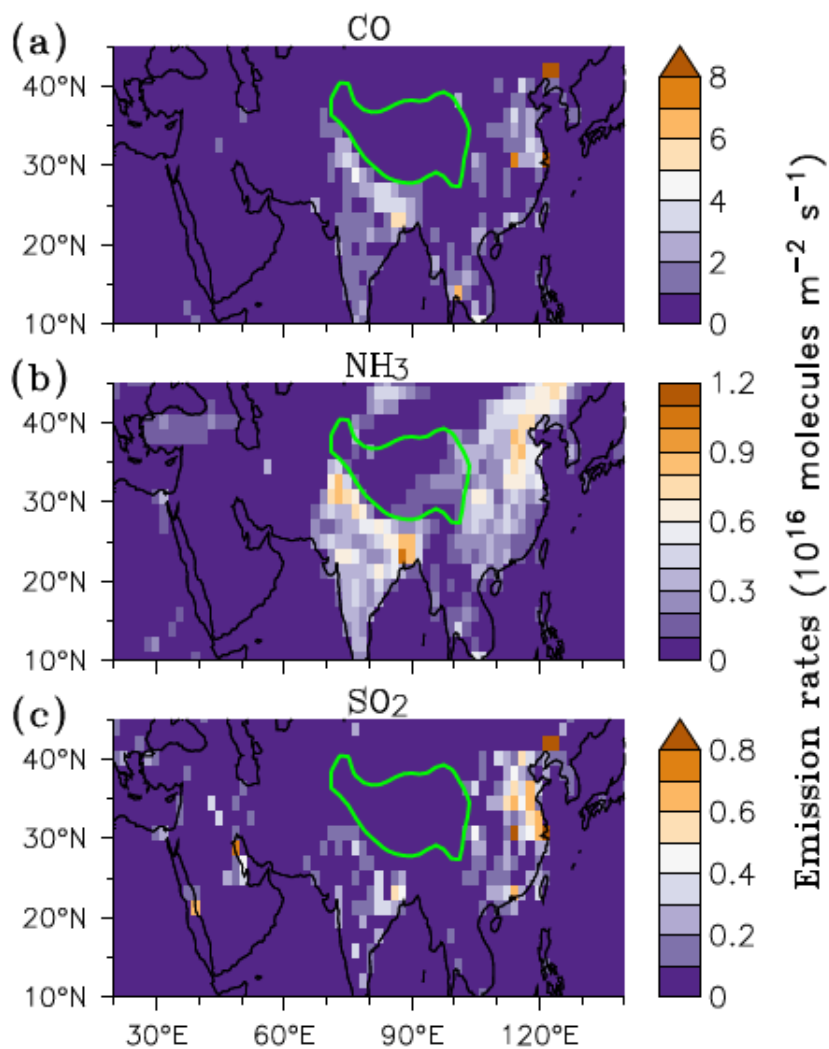


**Figure S2.** Anthropogenic emission rates of CO (a), NH<sub>3</sub> (b) and SO<sub>2</sub> (c) near the Earth's surface, averaged for JJA over the years 2010-2020, based on the CAMS emission inventory v4.2 (with a horizontal resolution of 0.5° longitude by 0.5° latitude) and interpolated to the EMAC model grid of T63 (with a horizontal resolution of 1.875° longitude by 1.875° latitude) used for this study. Green lines represent the 3 km terrain contour, highlighting the Tibetan Plateau.

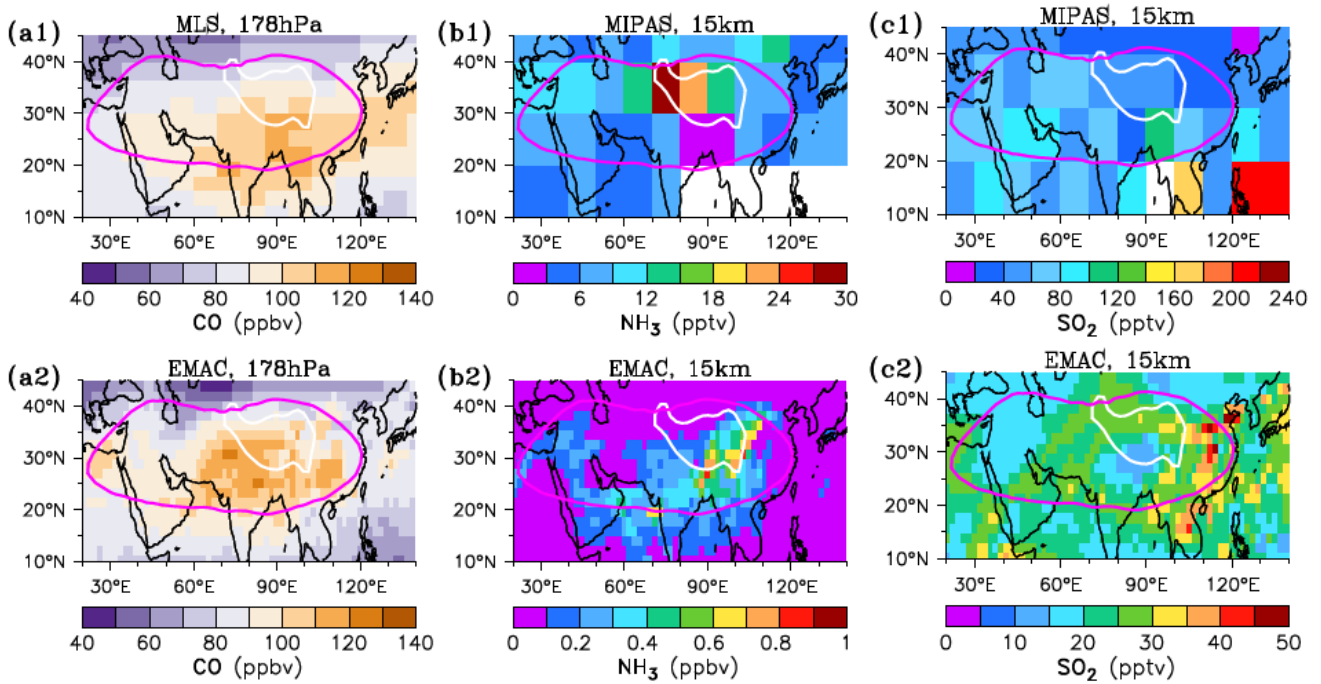


**Figure S3.** Comparisons of EMAC simulated cloud-free CO (**a2**) with MLS observed CO (**a1**) at 178 hPa and EMAC simulated cloud-free NH<sub>3</sub> (**b2**) and SO<sub>2</sub> (**c2**) with MIPAS observed NH<sub>3</sub> (**b1**) and SO<sub>2</sub> (**c1**) at 15 km above sea level for JJA 2010. Purple lines show the 16.64 km geopotential height contour at 100 hPa, highlighting the main ASMA area. White lines represent the 3 km terrain height contour, highlighting the Tibetan Plateau. White grid cells in (**b1**) and (**c1**) indicate the default values in MIPAS dataset.

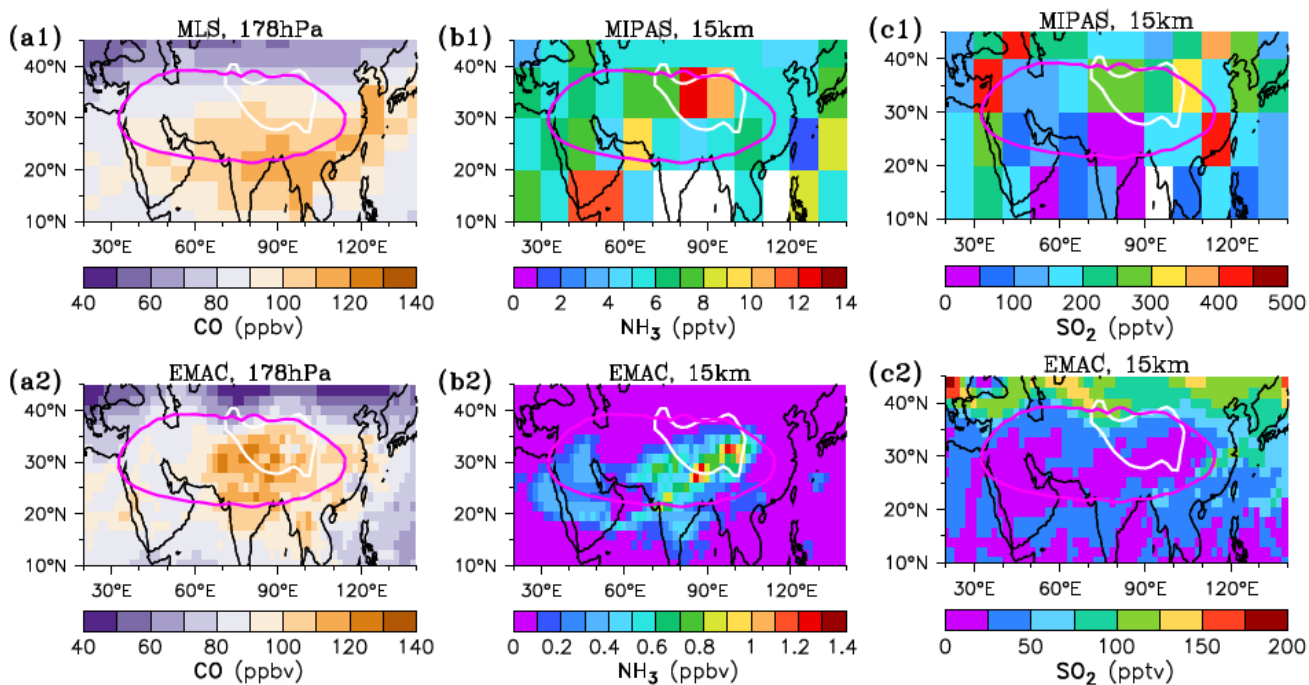


**Figure S4.** Same as Figure S3, but for JJA 2011.

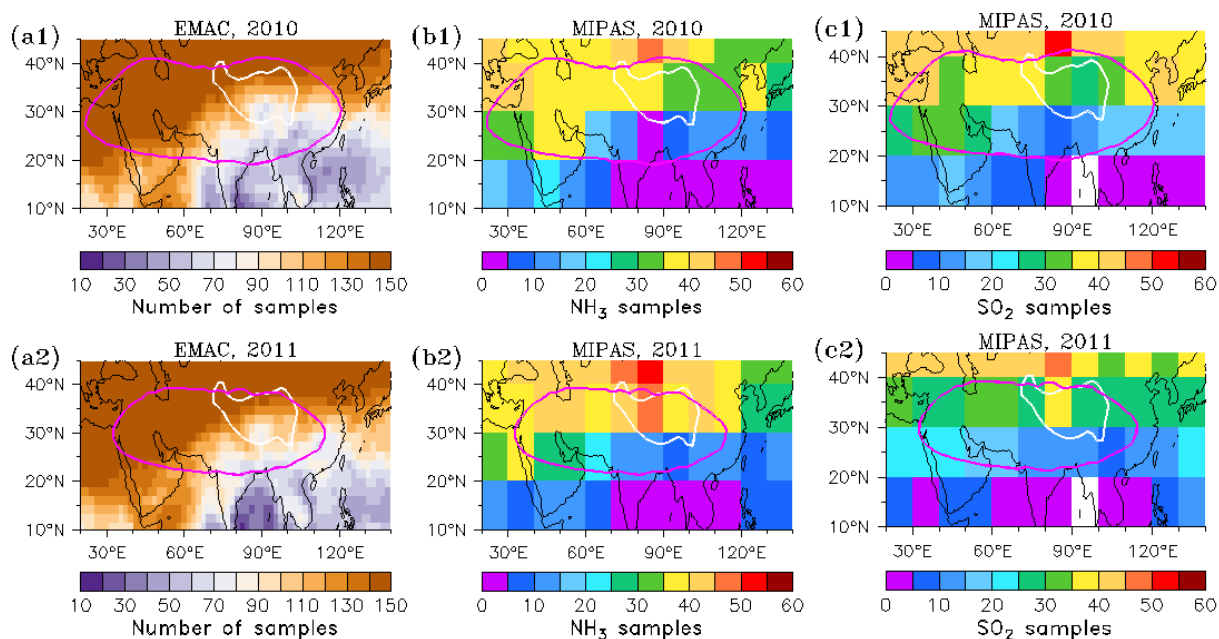


**Figure S5.** Number of samples for the cloud-free conditions in EMAC simulations at 5-h intervals (**a1** and **a2**) and for MIPAS  $\text{NH}_3$  (**b1** and **b2**) and  $\text{SO}_2$  (**c1** and **c2**) satellite measurements at 15 km above sea level for JJA in 2010 (**a1**, **b1**, and **c1**) and 2011 (**a2**, **b2**, and **c2**). Purple lines show the 16.64 km geopotential height contour at 100 hPa, highlighting the main ASMA area. White lines represent the 3 km terrain height contour, highlighting the Tibetan Plateau. White grid cells in (**c1**) and (**c2**) indicate the default values in MIPAS dataset.

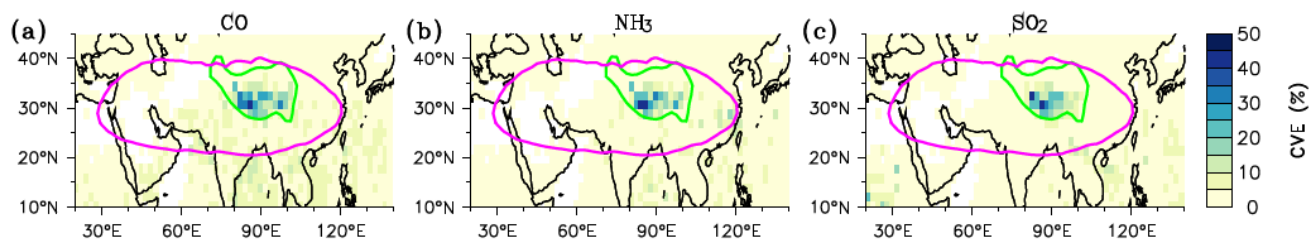


**Figure S6.** EMAC simulated averages of the deep convective transport efficiency (CVE) at 14 km, i.e., the ratio of the updraft mass flux (UMF) at 14 km height above sea level to its maximum in each deep convection column (expressed in percent, for CO (a), NH<sub>3</sub> (b) and SO<sub>2</sub> (c), in JJA during the years 2010-2020. Purple lines show the 16.64 km geopotential height contour at 100 hPa, highlighting the main ASMA area (see Figure S1). Green lines represent the 3 km terrain height contour, highlighting the Tibetan Plateau.

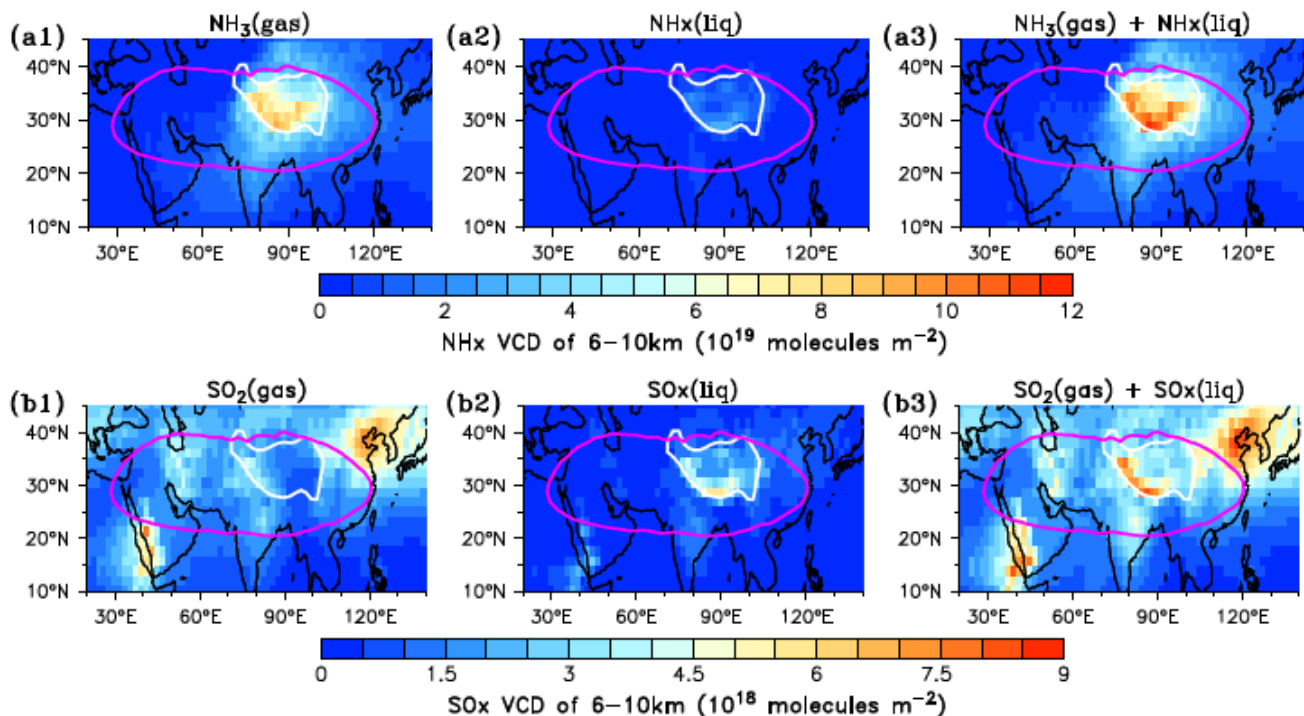


**Figure S7.** EMAC simulated vertical column densities (VCD) of gas-phase (**a1** and **b1**), liquid-phase (**a2** and **b2**) and gas-plus liquid- phase (**c1** and **c2**) within a height range of 6-10 km above sea level for  $\text{NH}_3$  and its reaction products in the clouds (denoted by  $\text{NH}_x$ ) (**a1**, **a2** and **a3**) and  $\text{SO}_2$  and its reaction products in the clouds (denoted by  $\text{SO}_x$ ) (**b1**, **b2** and **b3**), averaged for JJA over the years 2010-2020. Purple lines show the 16.64 km geopotential height contour at 100 hPa, highlighting the main ASMA area (see Figure S1). White lines represent the 3 km terrain height contour, highlighting the Tibetan Plateau. The  $\text{NH}_x$  in the clouds is the sum of liquid ammonia and ammonium, i.e.,  $\text{NH}_x(\text{liq}) \equiv \text{NH}_3(\text{liq}) + \text{NH}_4^+(\text{liq})$ . The  $\text{SO}_x$  in the clouds is the sum of liquid  $\text{SO}_2$  and its dissociation and oxidation products (denoted by  $\text{S}(\text{IV}, \text{liq})$  and  $\text{S}(\text{VI}, \text{liq})$ ), i.e.,  $\text{SO}_x(\text{liq}) \equiv \text{S}(\text{IV}, \text{liq}) + \text{S}(\text{VI}, \text{liq})$ , where  $\text{S}(\text{IV}, \text{liq}) \equiv \text{SO}_2(\text{liq}) + \text{HSO}_3^-(\text{liq}) + \text{SO}_3^{2-}(\text{liq})$  and  $\text{S}(\text{VI}, \text{liq}) \equiv \text{H}_2\text{SO}_4(\text{liq}) + \text{HSO}_4^-(\text{liq}) + \text{SO}_4^{2-}(\text{liq})$ .

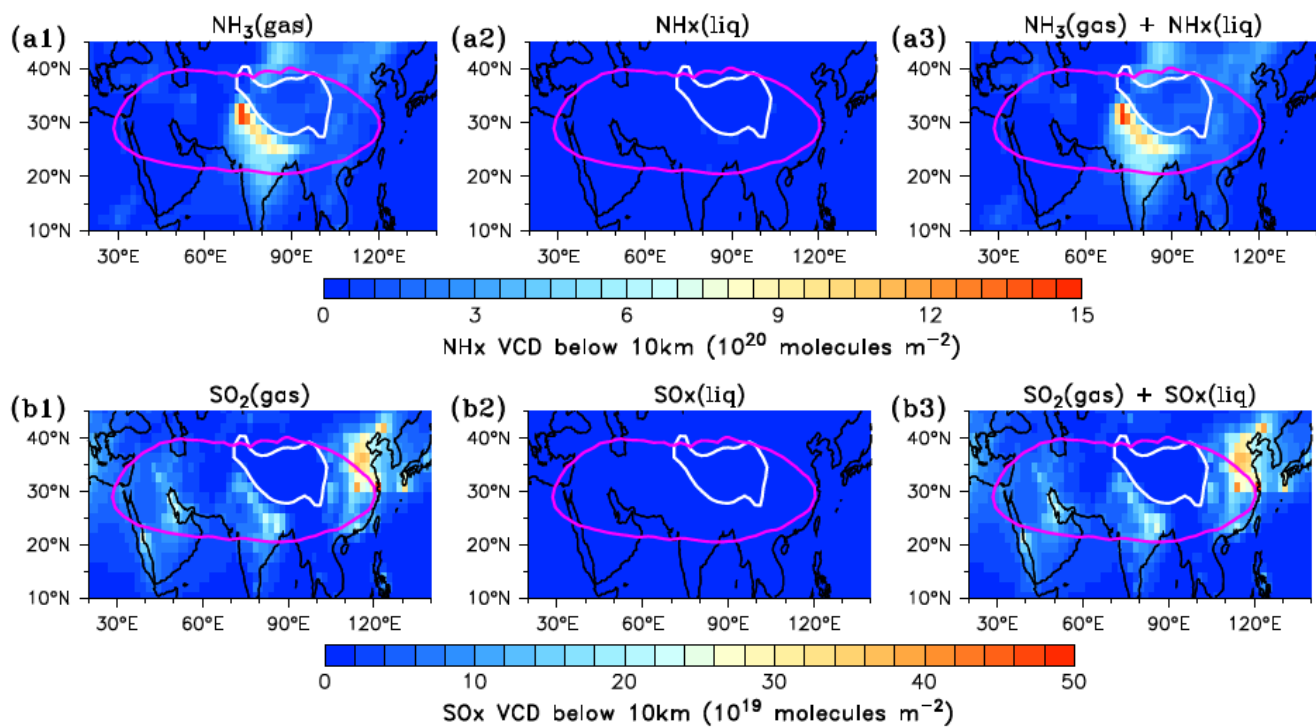


**Figure S8.** Same as Figure S7, except for a height range from the Earth's surface to 10 km above sea level.